STUDIA UBB PHYSICA, Vol. 60 (LX), 2, 2015, pp. 13-24
(RECOMMENDED CITATION)

SPECTROSCOPIC PROPERTIES OF CERIUM-BORO-BISMUTHATE GLASSES

M. BOSCA[1*], V. POP, E. CULEA, I. VIDA-SIMITI

ABSTRACT. X-Ray diffraction (XRD), density measurements, Fourier transform infrared (FTIR), diffuse reflectance ultraviolet–visible (DR-UV-Vis) and photoluminescence (PL) spectroscopies were performed on the glasses in the $xCeO_2 \cdot (100-x)[4Bi_2O_3 \cdot B_2O_3]$ system, with $0 \le x \le 15$ mol%, in order to point out the effect of CeO_2 addition to the boro-bismuthate host glass matrix on the local structure, optical and luminescent properties. The XRD patterns confirm a long-range structural disorder characteristic of amorphous network. FT-IR spectroscopy reveals absorption bands which are characteristic of BiO_3, BiO_6, BO_3 and BO_4 structural units. The optical band gap values for the studied glasses were calculated from the DR-UV-Vis spectra. The peaks evidenced by PL spectroscopy measurements are due to the presence of bismuth, in different valence states, in the studied glasses. Luminescence data show that the peaks intensity decrease over a content of 5 mol% CeO_2, this concentration representing the critical value over which the luminescence quenching becomes important.

Keywords: *Boro-bismuthate glasses; Cerium ions; XRD; FTIR; Optical and luminescent properties.*

INTRODUCTION

In recent technological world, glass materials doped with rare earth (RE) ions play an important role due to their multiple applications such as optical data transmission, detection, and information processes, undersea cameras, data storage, display technology, sensing (gas sensors, temperature sensors, etc.), laser technologies, producing low temperatures via magnetic cooling, etc. [1, 2]. Also, because a greater part of rare earths ions have an incomplete 4f level and can exhibit electronically forbidden f–f spectra in the ultraviolet, visible or infrared

[1] *Technical University of Cluj-Napoca, 103-105 Muncii Avenue, 400641 Cluj-Napoca, Romania*
[*] *Corresponding author e-mail: Maria.Cleja@phys.utcluj.ro*

region, the optical properties of the glasses doped with this kind of rare earths ions are very important.

Cerium dioxide (CeO_2) containing compounds have been used in various applications such as catalysts, solar cells, oxygen sensors, fuel cells, UV blocks, and polishing materials [3-5], likewise this oxide of cerium has useful properties such as hardness, greater stability at high temperatures, high absorption capacity of UV radiation and good optical and magnetic properties [4, 6]. Due to these interesting properties glasses doped with cerium oxide are also promising materials for optical and emitting devices [7-9].

On the other hand, glasses containing heavy metals like bismuth, are very important because can exhibit near-infrared luminescence, high density, high optical properties, high polarizability [10-12] and for these reasons have multiple applications such as optical amplifiers, optical fibers, electronic devices, thermal and mechanical sensors, reflecting windows, etc. Bismuth trioxide is not known like a glass former but in the presence of B_2O_3, P_2O_5, SiO_2, can became a glass network former because the Bi^{3+} ions are highly polarizable and therefore bismuth atom can exhibit various valence state. The glass networks containing bismuth ions can consist of BiO_6 octahedral and BiO_3 pyramidal units [13-15].

The boron trioxide is one of the classical glass formers. According to the literature [16-19] the structure of glasses containing boron trioxide consists of multiple boroxol rings and BO_3 and BO_4 units linked together by B-O-B bridges. This kind of glasses present also a great variety of applications being used as dielectrics and insulating materials. Their thermosluminescent properties are of a great interest, too [20].

Due to all these reasons, in this paper was considered the $4Bi_2O_3{\cdot}B_2O_3$ glass matrix to be a very interesting host for the cerium ions. The aim of this work was to investigate and establish the structural changes induced by the cerium oxide addition and to study the optical, structural and luminescent properties of this kind of glasses.

EXPERIMENTAL

Reagent grade purity Bi_2O_3, H_3BO_3 and CeO_2 were taken in suitable proportions to prepare the glasses from the $xCeO_2{\cdot}(100\text{-}x)[4Bi_2O_3{\cdot}B_2O_3]$ system. The required amounts of mentioned oxides were milled in an agate ball mil to obtain a fine powder. The obtained mixtures were melted for 20 minutes, using sintered corundum crucibles in an electric furnace at 1200 °C. The crucibles were placed into the electric furnace directly at this temperature. The glass samples were obtained by pouring the molten material onto a stainless–steel plate.

The XRD measurements of fine powdered sample were performed with a Shimadzu 6000 XRD diffractometer, in the 2θ range of 10 – 60° at a scan rate of 2°

per minute. The diffraction patterns were recorded at the room temperature using Cu-Kα radiation with the source power of 40 kV and 30 mA.

The density of samples was determined at room temperature using Archimede's method with distillate water as immersion liquid. The molar volume was calculated from the obtained density using the $V_m = M/\rho$ relation, where M is the molar mass of the sample and ρ is the density of the sample.

The FT-IR absorption spectra of the investigated glasses were registered at room temperature in the 400 - 1500 cm-1 range using a JASCO FT-IR 6200 spectrometer. The studied samples were mixed with KBr in a ratio of 2:300 glass powder: KBr, respectively.

The DR-UV-Vis spectra were recorded with a PerkinElmer Lambda 45 UV-Vis spectrometer equipped with an integrating sphere, at room temperature. The studied samples were measured in MgO pellets. DR-UV–Vis spectra of the investigated glasses were recorded in reflectance units and were transformed in Kubelka–Munk remission function F(R).

The photoluminescence (PL) spectra were registered at room temperature with a Jasco FP-8200 spectrofluorometer using a Xe lamp as excitation source. In order to obtain powders with similar dimensions the obtained glasses have been crushed and sieved. The excitation wavelength was 380 nm.

RESULTS AND DISCUSSION

XRD data

The amorphous nature of the prepared samples was examined using the XRD technique. The XRD patterns recorded for the investigated samples are shown in Fig. 1.

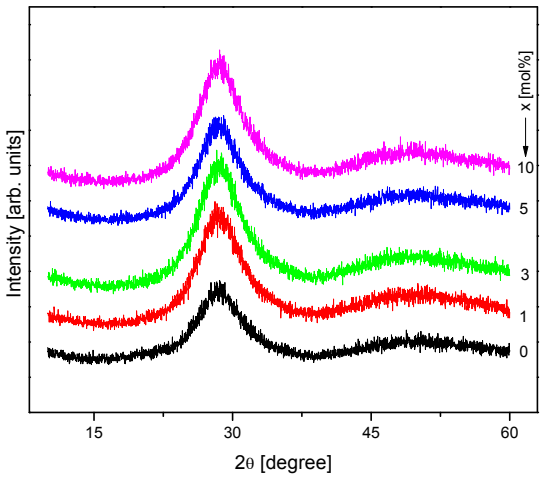

Fig. 1. XRD patterns of $xCeO_2 \cdot (100\text{-}x)[4Bi_2O_3 \cdot B_2O_3]$ glasses

The XRD patterns exhibit two broad diffuse scattering instead of crystalline peaks. The absence of sharp Bragg peaks in the XRD patterns confirms a long-range structural disorder characteristic of amorphous network. For all studied glasses the angular position for first amorphous halo is at about 28.60^0. From the first halo maximum position it can be calculated the average distance between the atoms in the first coordination sphere by using the relation $R = (5\lambda)/ (8 \sin\theta)$ [21]. For all investigated samples this distance was found to be about 3.89 Å.

Density and molar volume data

Fig. 2 presents the density (ρ) and molar volume (V_m) variations with increasing of CeO_2 content for the $xCeO_2 \cdot (100\text{-}x)[4Bi_2O_3 \cdot B_2O_3]$ glass system.

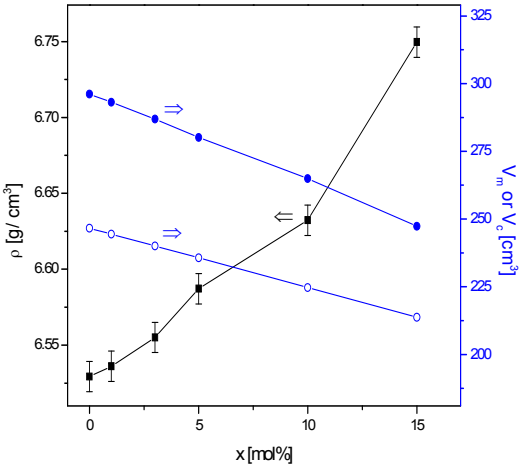

Fig. 2. Composition dependence of crystalline (○) and glassy (●) molar volume and of density (■) of $xCeO_2 \cdot (100\text{-}x)[4Bi_2O_3 \cdot B_2O_3]$ system

This figure shows that the density increases with increasing of CeO_2 content suggesting that the glass network becomes more compact. Fig. 2 shows also the calculated sums of the theoretical molar volumes (V_c) of the component oxides for the studied glasses considered in their crystalline states. The molar volume of the studied $xCeO_2 \cdot (100\text{-}x)[4Bi_2O_3 \cdot B_2O_3]$ glasses is always greater than that of their hypothetical crystalline oxide mixtures, indicating the presence of an excess structural volume in the glasses. On the other hand, the increase of cerium oxide content leads to a decrease of both the molar volume and the difference between V_m and V_c. These results show a better packing of coordination polyhedra in the structural network of boro-bismuthate glasses once with increasing of cerium ions content.

FTIR data

Fig. 3 shows the FTIR absorption spectra of the studied boro-bismuthate glasses doped with CeO_2.

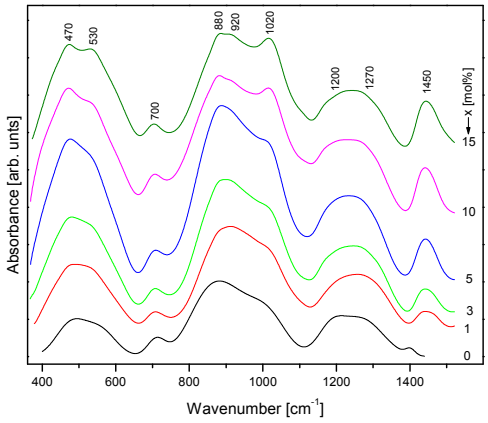

Fig. 3. FTIR spectra of $xCeO_2 \cdot (100\text{-}x)[4Bi_2O_3 \cdot B_2O_3]$ glasses

It can be observed the presence of three broad bands in the 400-650 cm^{-1}, 650-1100 cm^{-1} and 1100-1500 cm^{-1} spectral regions, respectively. These broad bands are the result of the overlapping of several individual bands. Each individual band gives information about the type of vibration and the concentration of a specific structural group. A deconvolution process was performed to extract the band centers, C, and its relative area, A, for each individual band. Fig. 4 presents the deconvoluted spectrum, in Gaussian bands, of the glass containing 15 mol% CeO_2, as representative example. Table 1 summarizes the bands assignment for the studied glasses.

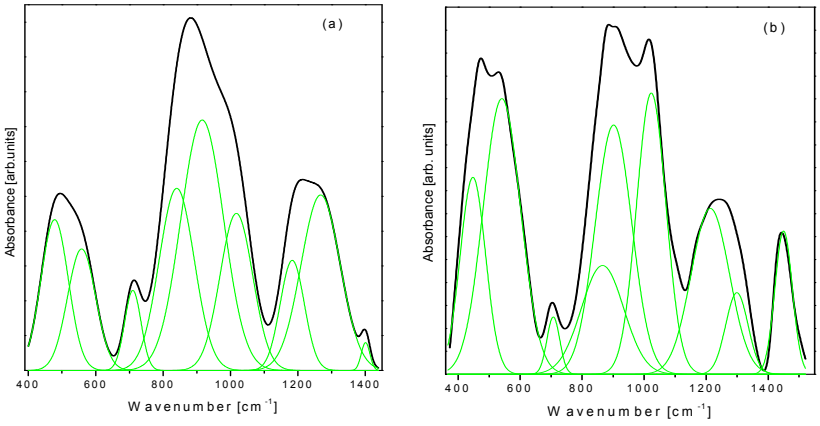

Fig. 4. Deconvoluted FTIR spectra of $xCeO_2 \cdot (100\text{-}x)[4Bi_2O_3 \cdot B_2O_3]$ glasses using a Gaussian type function for x = 0 mol% (a) and x = 15 mol% (b)

In the first spectral region, 400 - 650 cm^{-1}, the result of absorption band deconvolution indicates a number of 2 peaks. For the host glass matrix these bands are centered at ~ 478 and ~ 558 cm^{-1}. These bands were ascribed to the Bi-O bending vibration in BiO_3 units (the absorption band from ~ 478 cm^{-1}) and respectively in BiO_6 units (the band from ~ 558 cm^{-1}) [22-25]. As result of the appearance of cerium ions in the glass matrix, the intensity of these bands increase having a maximum for the glasses containing 5 mol% CeO_2 for the band from ~ 478 cm^{-1} and 10 mol% CeO_2 for the band from ~ 558 cm^{-1}. For higher CeO_2 contents the intensity of these bands decreases and shifts to lower wavenumbers, at ~ 447 and ~ 541 cm^{-1}, respectively.

In the second spectral region, 650 -1100 cm^{-1}, after deconvolution, the following bands located at ~ 710, ~ 840, ~ 916 and ~ 1017 cm^{-1} were obtained. The band from ~ 710 cm^{-1} was assigned to the bending vibrations of B-O-B linkage in the borate network [26-30]. The existence of this band was assumed to point out that at least some super-structural borate units are retailed in the structure of boro-bismuthate glasses [12]. The amplitude of this band is approximately the same for all the compositional range.

Table 1. Assignment of the IR bands for the $xCeO_2 \cdot (100\text{-}x)[4Bi_2O_3 \cdot B_2O_3]$ glasses

Wavenumber [cm^{-1}]	Assignments
454-478	Bi-O bend in BiO_3 units
541-558	Bi-O bend in BiO_6 units
706-710	B-O-B bend
840-859	Bi-O_{sym} stretch in BiO_3 units Bi-O vibration in distorted BiO_6 units
900-918	B-O stretch in BO_4 units from di-borate groups
1009-1026	B-O stretch in BO_4 units from tri-, tetra- and penta-borate groups
1183-1215	B–O^-_{asym} stretch in BO_3 units from pyro- and ortho-borate groups
1267-1297	B-O stretch in BO_3 units from boroxol rings
1400-1449	B-O^- stretch in BO_3 units from varied types of borate groups

The absorption band at ~ 840 cm^{-1} was assigned to the Bi-O symmetrical stretching vibration in BiO_3 units [22]. When the CeO_2 content increases to 15 mol%, this band shifts to higher wavenumbers, around 865 cm^{-1}. This latter band was ascribed to vibrations of strongly distorted BiO_6 octahedral units [22-25]. The compositional evolution of this band suggests a conversion of the BiO_3 into BiO_6 units with the increase of the cerium ions content. Thus, the presence of cerium ions influences the surrounding of the Bi^{3+} cations favoring the formation of BiO_6 units. The absorption bands from ~ 916 and ~ 1017 cm^{-1} indicate the presence of the BO_4 structural units in the studied glasses [19]. Thus, the absorption feature from ~ 916 cm^{-1} can be due to the B-O stretching vibrations in BO_4 units from di-borate groups, while the band from ~ 1017 cm^{-1} was assigned to the B–O stretching vibrations in BO_4 units from tri-, tetra- and penta-borate groups [26-30].

In the third IR spectral region, from 1100 to 1500 cm^{-1}, three bands were obtained centered at ~ 1183, ~ 1267 and ~1400 cm^{-1}. This spectral region originates from the stretching vibration and asymmetric stretching vibrations of B-O and B-O^- bonds respectively, in borate triangular units, which are of the BO_3 and BO_2O^- type [19]. The band at ~ 1183 cm^{-1} was assigned to asymmetric stretching vibrations of B–O^- in BO_3 units from pyro- and ortho-borate [19]. Pyro- and ortho-borate groups contain a large number of non-bridging oxygen. The peak at around 1267 cm^{-1} can be due to stretching vibration of B-O in boroxol rings [26-30]. The band situated at around 1400 cm-1 is due to stretching vibrations of B–O^- in BO_3 units from various types of borate groups [26-30].

It is well know that the addition of a modifier oxide, such as CeO_2, can cause changes in the relative population of BO_3 and BO_4 structural units. The fraction of four-coordinated boron atoms, N_4, can be used to trace these changes with increasing the cerium ions content. The deconvolution technique can be used to obtain the N_4 values, because the concentration of the structural units is proportional to the relative area of its component band. N_4 is the ratio of the number of BO_4 units (the relative areas of component bands from 900-918, 1009-1026 cm^{-1}) to the number of BO_4 units plus the number of BO_3 units (the relative areas of component bands from 1183-1215, 1267-1299, 1400-1449 cm^{-1}) [24, 25, 31, 32].

For the studied glasses the dependence of N_4 on CeO_2 content is shown in Fig. 5. The obtained value of N_4 for the host glass matrix is 0.634. For glasses doped with CeO_2 the values of N_4 decrease from 0.632 to 0.461 when the content of CeO_2 increases from 1 to 15 mol%. For glasses with $x \leq 10$ mol% the four-coordinated boron atoms are favored in the investigated glass system in comparison with the three-coordinated ones. For higher CeO_2 contents the three-coordinated boron atoms became favored.

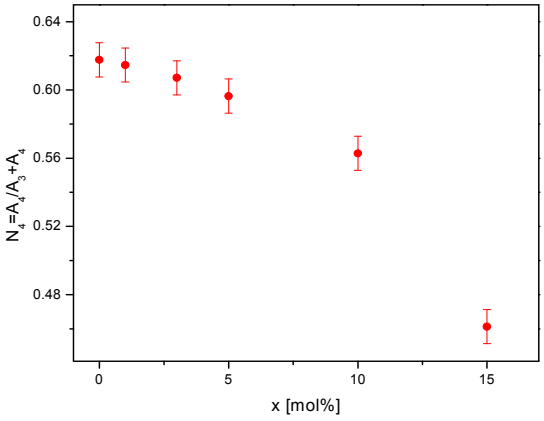

Fig. 5. The composition dependence of N_4 for the studied glasses

The structural changes observed in the network structure at the short-range order level by increasing the cerium ions content in the host glass matrix evidenced from FT-IR data suggest that the cerium ions play the role of vitreous network modifier in the investigated glasses.

DR-UV-Vis data

DR-UV–Vis spectra of the $xCeO_2 \cdot (100-x)[4Bi_2O_3 \cdot B_2O_3]$ glasses were recorded at room temperature in reflectance units and were transformed in Kubelka–Munk remission function F(R). The DR-UV-Vis spectra obtained for the studied glasses (after Kubelka–Munk transformation) are shown in Fig. 6a. From this figure it can be observed that our glasses exhibits no obvious absorption peaks in the 350-1000 nm wavelength range being in agreement with previously reported data [33]. The optical band gap energy, E_g, was calculated for all the studied samples by plotting $[F(R) \cdot h\upsilon]^2$ as a function of hυ, since F(R) is considered proportional to the radiation absorption (h is the Planck constant). Then, the E_g values were estimated by extrapolation of the linear region of the mentioned plots (see Fig. 6b).

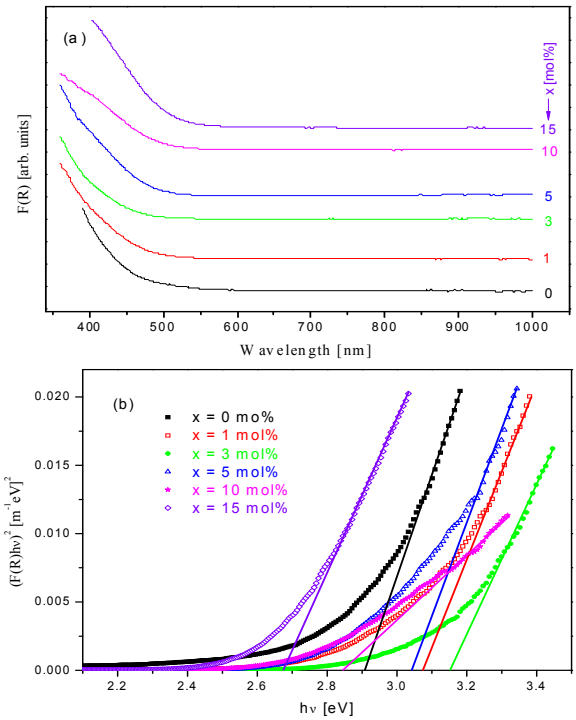

Fig. 6. DR-UV-Vis spectra of $xCeO_2 \cdot (100-x)[4Bi_2O_3 \cdot B_2O_3]$ glasses (a). Variation of $(F(R) \cdot h\upsilon)^2$ versus hυ for the studied glass samples (b).

Fig. 7 shows the composition dependence of E_g obtained for the studied glasses. The value of the optical band gap energy for the host glass matrix is 2.91 eV. For the glasses doped with cerium ions, we note the increase of the Eg values up to 3 mol% CeO_2. After that the E_g values decrease with increasing of CeO_2 content. The decrease of the optical band gap energy is due to the increase of the amount of non-bridging oxygen atoms from the glass network that occurs with increasing the cerium oxide content of the samples [34]. In the same time, as results from our FTIR data, the BO_4 tetrahedral borate units are converted in BO_3 trigonal units. This process generates an excess of oxygen that will determine the oxidation of cerium ions, $Ce^{3+} \rightarrow Ce^{4+}$, and the cerium ions are forced to have the maximum number of coordinated oxygen (eight). Such an assumption offers a reasonable explanation, as will be shown, that luminescent spectra do not exhibit significant luminescence peaks assignable to cerium.

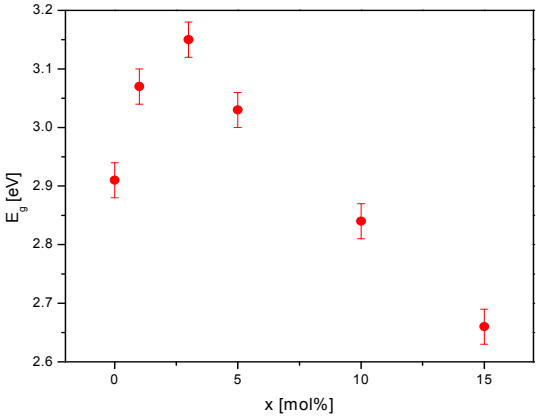

Fig. 7. Variation of E_g versus CeO_2 content for the $xCeO_2 \cdot (100\text{-}x)[4Bi_2O_3 \cdot B_2O_3]$ glasses

Finally, note that DR-UV–Vis data of the $xCeO_2 \cdot (100\text{-}x)[4Bi_2O_3 \cdot B_2O_3]$ glasses suggest that their glass network becomes more compact with increasing the cerium oxide content of the samples. This result supports the compositional evolution of density for the studied glasses.

Luminescence data

The luminescence spectra of the $xCeO_2 \cdot (100\text{-}x)[4Bi_2O_3 \cdot B_2O_3]$ glasses were recorded using an excitation wavelength of 380 nm. These spectra are presented in Fig. 8. The analysis of these spectra shows the presence of three emission bands (400 nm, 438 nm and 700 nm) that appear in all the samples, including the cerium

free sample. This observation suggests that the luminescent peaks may be assigned to the presence of bismuth ions, in different valence states, in all studied samples.

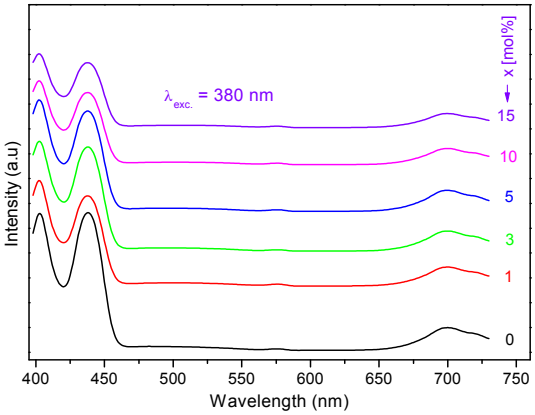

Fig. 8. Luminescence spectra of $xCeO_2 \cdot (100\text{-}x)[4Bi_2O_3 \cdot B_2O_3]$ glasses

The peaks around 400 nm and 438 nm were attributed to the Bi3+ ions, and are probably due to the $^3P_1 \rightarrow {}^1S_0$ transition and a $\pi^* \rightarrow \pi$ or $n \rightarrow \pi^*$ intraligand transition in polymetallate groups (BiO_3). This assumption is in agreement with literature data [35, 36]. The other peak, located around 700 nm, is due to presence of Bi^0 atoms in the studied samples [37]. Such atoms may appear in the glass network since the relatively high melting temperature (1200^0C) produces a thermal dissociation of Bi_2O_3 into elementary Bi.

Note that previous reports [7-9, 34] mentioned that in the 400-500 nm region and around 660 nm luminescence peaks appear due to the presence of Ce^{3+} ions. Note also that the Ce^{4+} ions do not show any luminescence response from 4f orbital which do not contain any electron [38]. The luminescent peaks of Ce^{3+} ions are due to the transitions from the 5d levels to the $^2F_{5/2}$ and $^2F_{7/2}$ ground state levels [7-9] and their number strongly depends on the Ce^{3+} ions environment [34]. In our luminescent spectra, these peaks overlap the peaks coming from the bismuth ions. The addition of cerium oxide produces changes of the luminescent peaks intensity but do not affect their position. The luminescent peaks intensity decreases by adding cerium oxide. Since this process becomes very intense over the 5 mol% cerium oxide content this value represents probably the one for which the luminescence quenching occurs.

CONCLUSIONS

Glasses from the $xCeO_2 \cdot (100\text{-}x)[4Bi_2O_3 \cdot B_2O_3]$ system with $0 < x > 15$ mol% were obtained by using the melt-quenching technique. XRD confirms the amorphous

nature of the studied samples. FT-IR spectra and the compositional variation of V_m and V_c reveal that CeO_2 acts as a structural network modifier and both Bi_2O_3 and B_2O_3 play the role of network formers. The FT-IR data show that the network structure of studied glasses consists of BiO_3, BiO_6, BO_3 and BO_4 units. The UV-Vis spectra show no absorption peaks in the 350-1000 nm wavelength range. The calculated optical band gap energy was observed to decrease for cerium oxide contents higher than 3 mol% suggesting that the glass network becomes more compact. These data are in agreement with density measurements. The luminescence data show that the peaks intensity decreases over a 5 mol% content of CeO_2 where the luminescence quenching becomes important.

ACKNOWLEDGMENT

This paper was supported by the Post-Doctoral Programme POSDRU/159/1.5/S/137516, project co-funded from European Social Fund through the Human Resources Sectorial Operational Program 2007-2013.

REFERENCE

1. B. Sun, H. Song, J. Wang, H. Peng, X. Zhang, S. Lu, J. Zhang and H. Xia, *Chem. Phys. Lett.,* 368, 412 (2003).
2. V. Venkatramu, P. Babu and C.K. Jayasankar, *Spectrochim. Acta A,* 63, 276 (2006).
3. X.D. Feng, D.C. Sayle, Z.L. Wang, M.S. Paras, B. Santora, A.C. Sutorik, T.X.T. Sayle, Y. Yang, Y. Ding, X.D. Wang and Y.S. Her, *Science,* 312, 1504 (2006).
4. A. Trovarelli, C. de Leitenburg, M. Boaro and G. Dolcetti, *Catal. Today,* 50, 353 (1999).
5. S.P. Singh, R.P.S. Chakradhar, J.L. Rao and B. Karmakar, *J. Alloys Compd.*, 493, 256 (2010).
6. E. Culea, L. Pop and M. Bosca, *J. Alloys Compd.,* 505, 754 (2010).
7. M. Rodriguez Chialanza, A. Cardenas, E. Castiglioni, J. Castiglioni, J.F. Carvalho and L. Fornaro, *J. Non-Cryst. Solids,* 401, 181 (2015).
8. P. Kaur, S. Kaur, G. P. Singh and D.P. Singh, *J. Alloy Compd.,* 588, 394 (2014).
9. Li-Hua Zheng, Xin-Yuan Sun, Ri-Hua Mao, Hao-Hong Chen, Zhi-Jun Zhang and Jing-Tai Zhao, *J. Non-Cryst. Solids*, 403, 1 (2014).
10. S. Hazra, S. Mandal and A. Ghosh, *Phys. Rev. B,* 56, 8021 (2005).
11. M. Nocun, W. Mozgawa, J. Jedlinski and J. Najman, *J. Mol. Structure,* 744-747, 603 (2014).
12. F.H. ElBatal, S.Y. Marzouk, N. Nada and S.M. Desouky, *Physics B,* 391, 88 (2007).
13. S. Hazra and A. Ghosh, *Phys. Rev. B,* 51, 851 (1995).
14. L. Baia, R. Stefan, J. Popp, S. Simon and W. Kiefer, *J. Non-Cryst. Solids,* 324, 109 (2003).
15. E. Culea, *J. Non-Cryst. Solids,* 357, 50 (2011).

16. D.L. Griscon, “Materials Science Research, Borate Glasses”, Plenum, New York, **1978**, pag. 36.
17. J. Krogh-Moe, *Phys. Chem. Glasses,* 3, 101 (1962).
18. R.L. Mozzi and B.E. Waren, *J. Appl. Crystallogr.,* 3, 251 (1970).
19. Y.D. Yiannopoulos, G.D. Chryssikos and E.I. Kamitsos, *Phys. Chem. Glasses,* 42, 164 (2001).
20. A.N. Yazici, M. Dogan, V.E. Kafadar and H. Toktamis, *Nucl. Instrum. Meth. Phys. Res. B, 2*46, 402 (2006).
21. H.P. Klug and L.E. Alexander, “X-Ray Diffraction Procedures“, Wiley, New York, **1970**, p. 632.
22. Y. Hu, N.H. Liu and U.L. Lin, *J. Mater. Sci.,* 33, 229 (1998).
23. R. Iordanova, V. Dimitriev, Y. Dimitriev and D. Klissurski, *J. Non-Cryst. Solids,* 180, 58 (1994).
24. P. Pascuta, G. Borodi and E. Culea, *J. Non. Cryst. Solids,* 354, 5475 (2008).
25. P. Pascuta, G. Borodi and E. Culea, *J. Mater. Sci.: Mater. Electron.,* 20, 360 (2011).
26. E.I. Kamitsos, M.A. Karakassides and G.D. Chyssikos, *J. Phys. Chem.,* 91, 1073 (1987).
27. M. Abo-Naf, F. H. ElBatal and M.A. Azooz, *Mater. Chem. Phys.,* 77, 846 (2002).
28. A. Kumar, S.B. Rai and D.K. Rai, *Mater. Res. Bull.,* 38, 333 (2003).
29. P. Pascuta and E. Culea, *Mater. Lett.,* 62, 417 (2008).
30. P. Pascuta, *J. Mater. Sci.: Mater. Electron.,* 21, 338 (2010).
31. K. El-Egili, *Physica B,* 325, 340 (2003).
32. P. Pascuta, L. Pop, S. Rada, M. Bosca and E. Culea, *J. Mater. Sci.: Mater. Electron.,* 19, 424 (2008).
33. Y.Q. Qiu, J. Kang, C.X. Li, X.Y. Dong and C.L. Zhao, *Laser Physics,* 20, 487 (2010).
34. P. Kaur, G. P. Singh, S. Kaur and D.P. Singh, *J. Mol. Structure,* 1020, 83 (2012).
35. K. Polak and E. Mihokova, *Opt. Mater.,* 32, 1280 (2010).
36. M. Feyand, M. Koppen, G. Friedrichs and N. Stock, *Chem. Eur. J.,* 19, 12537 (2013).
37. M. Peng, C. Zollfrank and L. Wondraczek, *J. Phys.: Condens. Matter,* 21, 285106 (2009).
38. G. K. Das Mohapatra, *Phys. Chem. Glasse*s, 39, 50 (1998).